

# UCSF

## UC San Francisco Previously Published Works

### Title

Zika Virus Nonstructural Protein 1 Disrupts Glycosaminoglycans and Causes Permeability in Developing Human Placentas.

### Permalink

<https://escholarship.org/uc/item/2pg5x6sz>

### Journal

The Journal of Infectious Diseases, 221(2)

### ISSN

0022-1899

### Authors

Puerta-Guardo, Henry  
Tabata, Takako  
Petitt, Matthew  
[et al.](#)

### Publication Date

2020-01-02

### DOI

10.1093/infdis/jiz331

Peer reviewed

# Zika Virus Nonstructural Protein 1 Disrupts Glycosaminoglycans and Causes Permeability in Developing Human Placentas

Henry Puerta-Guardo,<sup>1</sup> Takako Tabata,<sup>2</sup> Matthew Petitt,<sup>2</sup> Milena Dimitrova,<sup>1</sup> Dustin R. Glasner,<sup>1</sup> Lenore Pereira,<sup>2</sup> and Eva Harris<sup>1</sup>

<sup>1</sup>Division of Infectious Diseases and Vaccinology, School of Public Health, University of California, Berkeley; <sup>2</sup>Department of Cell and Tissue Biology, School of Dentistry, University of California San Francisco

**Background.** During pregnancy, the Zika flavivirus (ZIKV) infects human placentas, inducing defects in the developing fetus. The flavivirus nonstructural protein 1 (NS1) alters glycosaminoglycans on the endothelium, causing hyperpermeability in vitro and vascular leakage in vivo in a tissue-dependent manner. The contribution of ZIKV NS1 to placental dysfunction during ZIKV infection remains unknown.

**Methods.** We examined the effect of ZIKV NS1 on expression and release of heparan sulfate (HS), hyaluronic acid (HA), and sialic acid on human trophoblast cell lines and anchoring villous explants from first-trimester placentas infected with ZIKV ex vivo. We measured changes in permeability in trophoblasts and stromal cores using a dextran-based fluorescence assay and changes in HA receptor expression using immunofluorescent microscopy.

**Results.** ZIKV NS1 in the presence and absence of ZIKV increased the permeability of anchoring villous explants. ZIKV NS1 induced shedding of HA and HS and altered expression of CD44 and lymphatic endothelial cell HA receptor-1, HA receptors on stromal fibroblasts and Hofbauer macrophages in villous cores. Hyaluronidase was also stimulated in NS1-treated trophoblasts.

**Conclusions.** These findings suggest that ZIKV NS1 contributes to placental dysfunction via modulation of glycosaminoglycans on trophoblasts and chorionic villi, resulting in increased permeability of human placentas.

**Keywords.** Zika virus NS1; heparan sulfate; cytotrophoblast; Hofbauer cells; hyaluronic acid.

Zika virus (ZIKV) is a mosquito-borne flavivirus (*Flaviviridae* family) that in 2015–2016 caused massive epidemics in the Americas. ZIKV infection during pregnancy is associated with Zika congenital syndrome and with other neurological complications, such as Guillain-Barré syndrome, in adults [1, 2]. Our previous studies reported patterns of infection and elucidated routes by which ZIKV penetrates the placenta, leading to virus transmission [3, 4]. In the developing human placenta, a subset of specialized epithelial cells, cytotrophoblasts (CTBs), fuse, forming a layer of multinucleated syncytiotrophoblasts (STBs) that overlays CTBs, forming a barrier that covers chorionic villi. Syncytiotrophoblasts facilitate transport of substances from maternal blood to the fetal circulation and production of interferon lambda that prevents infection of the placental surface [5, 6]. Cytotrophoblasts also proliferate, forming cell columns that

anchor the placenta to the uterine wall and branch into villi that increase the surface for nutrient exchange [6]. We reported that proliferating CTBs in proximal cell columns and Hofbauer cells in villous cores, as well as primary umbilical vein endothelial cells, stromal fibroblasts, and amniotic epithelial cells isolated from fetal membranes, are targets for ZIKV replication, suggesting both placental and paraplacental routes of virus transmission [3, 4].

Flavivirus nonstructural protein 1 (NS1) plays a critical role in pathogenesis by increasing the permeability of endothelial cell monolayers in vitro as well as causing vascular leakage in vivo [7]. This hyperpermeability is mediated in part by disruption of the endothelial glycocalyx—a network of glycosaminoglycans (GAGs), proteoglycans, and sialic acid (Sia) expressed on the surface of human endothelial cells [8–10]. More important, increased circulating levels of these GAGs correlate with severe dengue disease in humans [11, 12]. However, the effect of ZIKV NS1 on the integrity of the placental barrier has not been addressed.

Glycosaminoglycans are polymers of unbranched repeating disaccharide units and are abundant in the extracellular matrix (ECM). The GAG family is composed of 5 members—hyaluronic acid (HA), heparan sulphate (HS), chondroitin sulphate (CS), dermatan sulphate, and keratan

Received 19 April 2019; editorial decision 17 June 2019; accepted 26 June 2019; published online June 27, 2019.

Presented in part: 67th Annual Meeting of the American Society of Tropical Medicine and Hygiene, October 28–November 1, 2018, New Orleans, LA.

Correspondence: Lenore Pereira, PhD, Department of Cell and Tissue Biology, University of California, San Francisco, 513 Parnassus Ave, San Francisco, CA 94143 (lenore.pereira@ucsf.edu).

The Journal of Infectious Diseases® 2020;221:313–24

© The Author(s) 2019. Published by Oxford University Press for the Infectious Diseases Society of America. All rights reserved. For permissions, e-mail: journals.permissions@oup.com. DOI: 10.1093/infdis/jiz331

sulphate—and their presence in all vertebrate tissues implicates their diverse importance and functions. Hyaluronic acid, the largest member of the GAG family, functions in physiological processes, including ovulation, fertilization, and inflammation. Heparan sulphate acts as an attachment factor for growth factors, chemokines, and complement components during normal physiological and immune functions, as well as for numerous viruses [13–15]. Sialic acid constitutes a family of monosaccharides with a nine-carbon backbone, typically found on terminating branches of N-glycans, O-glycans, and glycosphingolipids (gangliosides), and occasionally capping side chains of glycosylphosphatidylinositol anchors [16]. Given their location, ubiquitous distribution, and hydrophilicity, GAGs and Sia can modulate a wide variety of physiological functions, and modification of their density and integrity may lead to pathology [17].

Human placentas express a variety of GAGs, including an abundance of HA [18, 19]. Hyaluronic acid, a nonsulfated GAG, is a major component of the ECM and can serve as a ligand for cell surface receptors to stimulate cellular activities, most notably through its major receptor, CD44. CD44 is a transmembrane glycoprotein receptor that binds to HA and regulates cellular activities, such as proliferation, migration, and apoptosis, by triggering downstream signaling cascades [20]. In addition, lymphatic endothelial cells have a specific HA receptor, lymphatic endothelial cell HA receptor 1 (LYVE-1), that is also expressed by Hofbauer cells (macrophages in villus cores [21, 22]) and that mediates uptake of HA and promotes HA-mediated rolling of leukocytes [23].

In this study, we examined the effect of soluble NS1 from ZIKV and the related West Nile virus (WNV) on the expression of HS, HA, and Sia, 3 main components of the ECM in cell monolayers and tissues. In addition, we examined (1) the barrier function of human trophoblast monolayers *in vitro* using transepithelial electrical resistance (TEER) and (2) chorionic villous explants *ex vivo* from human placentas at different gestational ages (GAs) using a dextran-fluorescence-based assay. The integrity of ECM components and intercellular junction proteins and the expression of CD44 and LYVE-1, 2 main HA receptors, was examined by immunofluorescence assay (IFA), and the levels of soluble HA, HS, and Sia were quantified by enzyme-linked immunosorbent assay (ELISA). Finally, we examined the role of soluble ZIKV NS1 in explants exposed to preparations of ZIKV (unpurified vs purified) that contained different amounts of soluble NS1.

## MATERIALS AND METHODS

### Ethics Statement

Collection of human tissue samples for this study was approved by the Institutional Review Board of the University of California, San Francisco (Supplemental Methods).

### Cell Lines and Virus

For *in vitro* experiments, we used 2 human placental trophoblast-derived cell lines: JAR and JEG-3 cells (Supplemental Methods). ZIKV strain Nica 2–16 was isolated from a ZIKV-infected patient in Nicaragua in 2016 [3].

### Recombinant Nonstructural Protein 1

Recombinant NS1 proteins from ZIKV (Suriname Z1106033) and WNV (NY99) were produced in HEK293 cells by the Native Antigen Company (Oxfordshire, United Kingdom) and were certified to be endotoxin-free and more than 95% pure (see Supplemental Methods).

### Epithelial Permeability Assay

The effect of recombinant flavivirus NS1 proteins on epithelial permeability was evaluated by measuring the TEER of JAR cell monolayers grown on a 24-well Transwell polycarbonate membrane system (Transwell permeable support, 0.4  $\mu\text{m}$ , 6.5 mm insert; Corning Inc.) (Supplemental Methods).

### Fluorescence Permeability Assay in Chorionic Villous Explants *Ex Vivo*

The effect of soluble NS1 proteins on the barrier function of human chorionic villi was evaluated using a dextran-fluorescence permeability assay in chorionic villi isolated from human placentas (7–14 weeks GA) (Supplemental Methods) [3, 8]. In addition, the effect of ZIKV on the permeability of anchoring villous explants was evaluated on individual explants infected with unpurified or purified preparations of ZIKV Nica 2–16 in 250  $\mu\text{L}$  DMEM/F12 medium, with or without exogenous ZIKV NS1 (5  $\mu\text{g}/\text{mL}$ ) (Supplemental Methods).

### Fluorescence Microscopy for Visualization of Glycosaminoglycans and Intercellular Junction Proteins

For imaging experiments, JAR and JEG-3 cells were grown on coverslips coated with collagen (500  $\mu\text{g}/\text{mL}$ ; Sigma) and imaged on a Zeiss LSM 710 Axio Observer inverted fluorescence microscope equipped with a 34-channel spectral detector. The integrity of GAG components and intercellular junction complexes was examined by IFA and confocal microscopy analysis (Supplemental Methods).

### Chorionic Villous Explant Embedding and Immunohistochemical Staining

After fixation and LI-COR imaging, explants were photographed on a Leica M125 stereoscope equipped with a Leica MC170-HD digital camera, frozen, embedded in gelatin, and sectioned (5  $\mu\text{m}$ ) as previously described [3, 4] (Supplemental Methods).

### Glycosaminoglycan and Sialic Acid Enzyme-Linked Immunosorbent Assays

Levels of soluble HA (R&D Systems), HS (LSBio), and Sia (Abcam) were measured from culture supernatants using ELISA assays following the manufacturer's instructions.

### Nonstructural Protein 1 Capture Enzyme-Linked Immunosorbent Assay

The levels of soluble NS1 in the ZIKV preparations were determined using an in-house capture ELISA as previously described [24] (Supplemental Methods).

### Statistical Analyses

Prism version 5.0 (GraphPad) was used for data analysis. Comparisons between 2 or >2 groups of data were performed by *t* test (nonparametric Mann-Whitney test) and ordinary one-way analysis of variance (ANOVA), respectively. Two-way ANOVA was used for multiple comparisons between groups. A *P* value of <.05 was considered statistically significant.

## RESULTS

### ZIKA NS1 modulates the integrity of GAGs on human trophoblast cell lines, inducing shedding and increasing permeability

In this study, we examine the effect of ZIKV NS1 and WNV NS1 on the integrity/expression of 2 GAGs, HS and HA, and the monosaccharide Sia on human trophoblast-derived cell lines (JAR, JEG-3). Analyses by IFA showed reduced staining for HS (~80%), Sia (~60%), and HA (~40%) on JAR cells 24 hours posttreatment (hpt) with ZIKV NS1 compared with untreated cells (Figure 1Ai–iii and B). Nonstructural protein from the closely related WNV flavivirus did not affect the expression of these components nearly as dramatically (Figure 1Ai–iii and B). A similar phenotype was detected on JEG-3 cells (Figure 1B, Supplementary Figure S1A–C) [25]. Significantly increased levels of HS, HA, and Sia were detected in the supernatant of JAR and JEG-3 monolayers treated with ZIKV NS1 compared with WNV NS1 and untreated cells (Figure 1Ci–iii). In addition, we assessed the cellular barrier function of trophoblasts treated with ZIKV or WNV NS1 proteins by measuring TEER [26]. We found that ZIKV NS1 (5 µg/mL) and tumor necrosis factor-α (10 ng/mL), an immunomodulatory and vasoactive molecule, significantly increased the permeability of JAR monolayers compared with treatment with WNV NS1 (5 µg/mL), which induced much smaller changes in TEER (Figure 2A). This barrier dysfunction correlated with altered distribution of ZO-1 (tight junction protein) and E-cadherin (adherens junction protein) on JAR cells treated with ZIKV NS1 (Figure 2Ci–iii) but not WNV NS1 (Figure 2Di–iii) or untreated cells (Figure 2Bi–iii). These results suggest that ZIKV NS1 alters the expression of GAGs on human trophoblasts, inducing their shedding into the extracellular milieu, and changes the distribution of key intercellular junction proteins, together leading to increased permeability and altered barrier function.

### Exogenous ZIKV NS1 increases the permeability of and release of GAGs from human anchoring villous explants

We recently showed that soluble NS1 from ZIKV increases permeability of human umbilical vein endothelial cells in vitro [7].

To determine whether NS1 permeabilizes differentiating anchoring villi, we tested the permeability of villous explants dissected from placentas of 7 to 14 weeks GA to Alexa-680-labeled dextran after exposure to recombinant ZIKV and WNV NS1 proteins (Figure 3A, Supplementary Figure S2). Treatment with ZIKV NS1 (5 µg/mL) led to consistently significantly greater mean permeability than untreated explants or treatment with WNV NS1 at the same concentration (Figure 3B). In some explants, the permeability after treatment with WNV NS1 was higher than untreated explants; however, no significant increases were observed (Figure 3B). It is noteworthy to mention that greater permeability was seen in villous explants exposed to ZIKV NS1 but not WNV NS1 at GAs 7 and 9 weeks, compared to 10 and 14 weeks (*P* = .0009; *P* = .0154). In addition, treatment of chorionic villous explants with ZIKV NS1 led to increased levels of soluble HS and HA compared with untreated explants and WNV NS1-treated explants (Figure 3Ci and ii). In contrast, levels of Sia were not affected in any of the experimental conditions (Figure 3Ciii). Together, these data suggest that ZIKV NS1 increases the permeability of anchoring villi in early gestation and modulates shedding of HS and HA from chorionic villi, leading to hyperpermeability *ex vivo*.

### ZIKA in the presence of soluble ZIKV NS1 causes hyperpermeability of anchoring villous explants, degradation of HA, and increased levels of CD44 on villous stromal cells

Next, we compared the effects of ZIKV NS1 on the permeability of anchoring villous explants in the presence of ZIKV using an isolate from the Americas (Nica 2–16) [3] (Figure 4A). Nica 2–16 was grown in C6/36 cells (*Aedes albopictus*), and the cell-free supernatant was used directly to infect chorionic villous explants (unpurified ZIKV). As shown above, NS1 alone altered the permeability of anchoring villi (Figure 3A and B). Because NS1 is secreted by flavivirus-infected cells, we used a purified preparation of ZIKV (purified ZIKV) to determine the effect of the soluble NS1 in unpurified virus preparations on villus permeability. We first measured the levels of free NS1 in both preparations and found that the unpurified stock of ZIKV contained significantly higher levels of soluble NS1 (2823 ± 245 µg/mL) than the purified virus (583 ± 154 µg/mL) (Supplementary Figure S3). Permeability experiments on villous explants showed consistent differences in permeability of villi exposed to unpurified and purified ZIKV (*P* < .0085) (Figure 4B, red bars). Furthermore, explants exposed to purified ZIKV in the presence of exogenous ZIKV NS1 also led to consistently greater permeability than exposure to purified ZIKV alone (*P* < .0331) (Figure 4B). The mean permeability measured for villous explants treated with purified ZIKV was similar to the levels in control (untreated and uninfected) explants (Figure 4B).

Based on the ability of ZIKV NS1 to modulate the expression of GAGs on trophoblast cells, we examined release of HA from anchoring villous explants infected in the presence

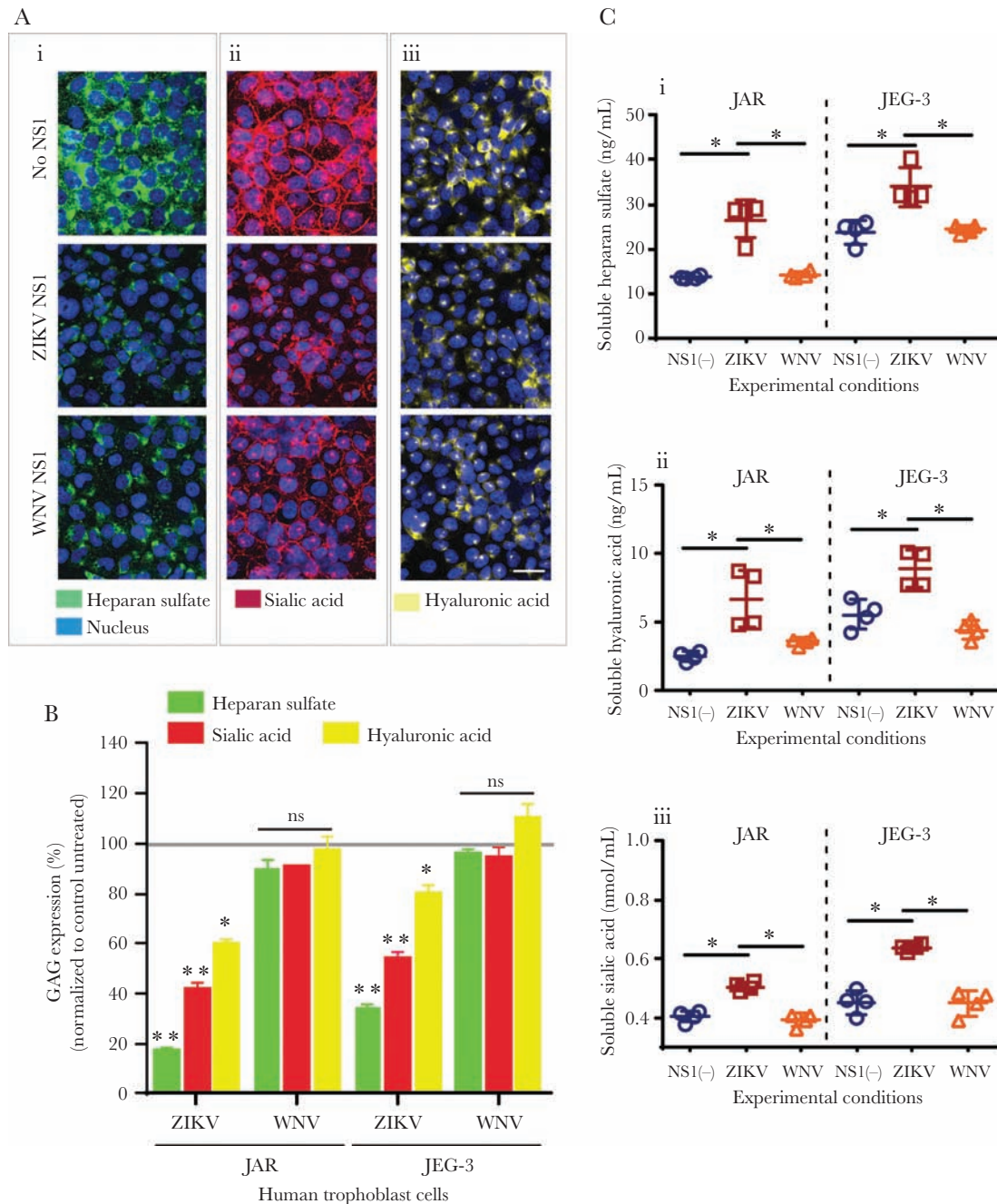


**Figure 1.** Zika virus (ZIKV) NS1 induces shedding of glycosaminoglycans (GAGs) from human trophoblast cells. (A) Immunofluorescence staining of (i) heparan sulfate [HS], (ii) sialic acid [Sia], and (iii) hyaluronic acid [HA] in confluent monolayers of JAR cells cultured on collagen-treated glass cover slips after 24 hours of treatment with ZIKV NS1 Suriname (5  $\mu\text{g}/\text{mL}$ ) or West Nile virus (WNV) NS1 (5  $\mu\text{g}/\text{mL}$ ). Images are representative of 4 independent experiments run in duplicate. Magnification,  $\times 20$ . Scale bar = 10  $\mu\text{m}$ . (B) Mean fluorescence Intensity analyses of GAG expression on JAR monolayers after ZIKV or WNV NS1 treatment as described above. Each bar shows the mean  $\pm$  standard error (SE) of 4 independent experiments processed in duplicate. The percentage of GAG expression on JAR and JEG cells treated with NS1 was normalized to the control untreated cells taken as 100%. (C) Enzyme linked immunosorbent assay quantification of soluble (i) HS, (ii) HA, and (iii) Sia in the supernatants obtained from JAR and JEG-3 cells 24 hours posttreatment with ZIKV (open squares) or WNV NS1 (open triangles) proteins (5  $\mu\text{g}/\text{mL}$ ). Untreated cells (open circles). Data were derived from 4 independent experiments and were analyzed by nonparametric Mann-Whitney analysis. \*,  $P < .05$ . Magnification,  $\times 20$ . Scale bar = 10  $\mu\text{m}$ . ns, not significant.

or absence of free NS1 in the medium and compared these values to the permeability measurements of the same explants (Figure 4Bi–iii, orange bars). As with the permeability values, the levels of HA released into the medium were

higher in villous explants infected with unpurified ZIKV and explants infected with purified ZIKV in the presence of exogenous ZIKV NS1 than in either control untreated/uninfected explants or explants infected with purified ZIKV

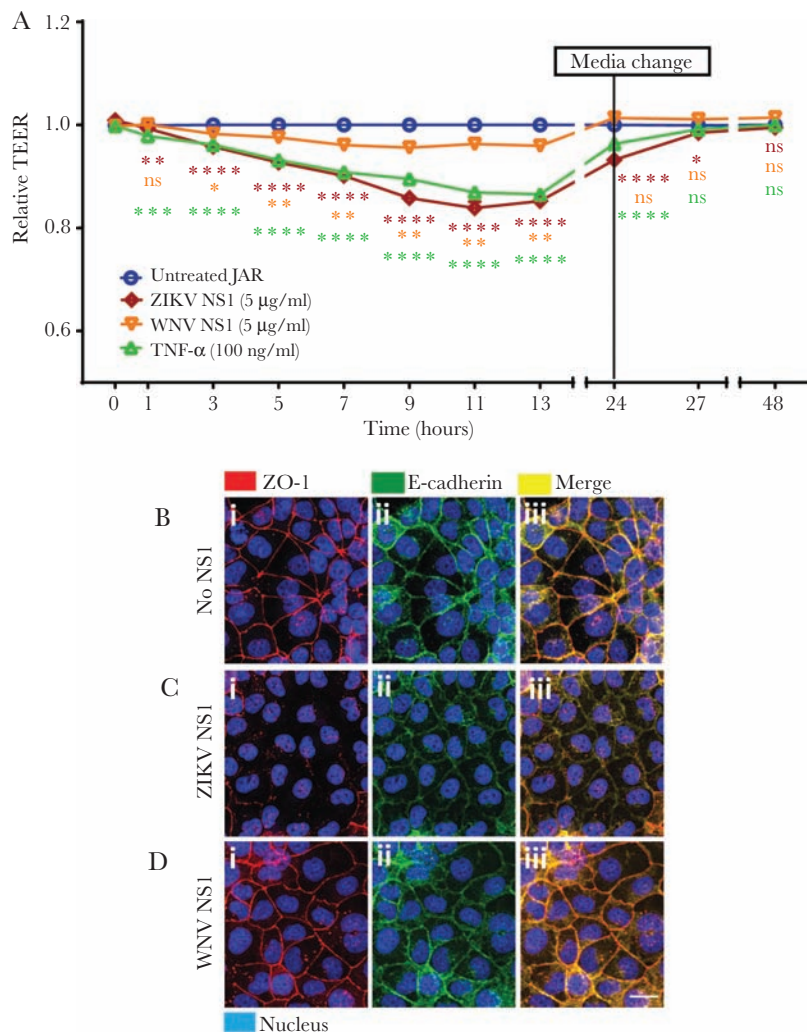


**Figure 2.** Zika virus (ZIKV) NS1 modulates permeability and integrity of the intercellular junction complex of human trophoblast monolayers in vitro. (A) Permeability of JAR cells cultured on Transwell inserts determined by transepithelial electrical resistance (TEER) assay in the presence of ZIKV or West Nile virus (WNV) NS1 proteins (5 µg/mL) added to the apical chamber. Untreated cells were used to establish a resistance baseline. Tumor necrosis factor (TNF)-α (10 ng/mL) was used as a positive control for reducing TEER values. Transepithelial electrical resistance was measured for 48 hours, every 2 hours from 1–13 hours, and permeability was expressed as relative TEER of experimental conditions compared with untreated controls. Each line represents the mean ± standard deviation of 3 independent experiments. Statistical analyses were performed by multiple comparisons between groups and untreated cells using two-way analysis of variance. Significant differences were considered as  $P < .05$ . (B, C, and D) Integrity of intercellular junctional complexes was evaluated by immunofluorescence assay on JAR cells exposed to ZIKV or WNV NS1 proteins (5 µg/mL) 12 hours posttreatment. ZO-1, a tight junction protein (red), and E-cadherin, an adherens junction protein (green), were visualized on JAR monolayers cultured on glass coverslips by confocal microscopy ( $n = 2$ ). (i) Control, (ii) ZIKV NS1, and (iii) WNV NS1. Magnification,  $\times 20$ . Scale bar = 10 µM. ns, not significant.

alone. Because increased levels of released HA could modulate cellular receptors CD44 and LYVE-1 [23, 27], we next examined their expression by immunofluorescence in sections of anchoring villi treated with unpurified ZIKV or purified ZIKV ± exogenous ZIKV NS1 as described above. We found consistent and substantial changes in staining for CD44 and LYVE-1 on stromal fibroblasts in cores of villi infected with unpurified ZIKV compared with purified ZIKV (Figure 4Ci–v). We also noted that exposure of explants to purified ZIKV in the presence of exogenous ZIKV NS1 also resulted in increased levels of CD44 on stromal fibroblasts and decreased levels of LYVE-1 on Hofbauer cells in villous

cores compared with uninfected villi or those infected with purified ZIKV without exogenous NS1 (Figure 4Di–v). These results suggest that ZIKV NS1 induces release of HA, resulting in increased expression of CD44 and reduced expression of LYVE-1 in villous cores.

#### ZIKV NS1 Increases the Expression of Human Hyaluronidases on Trophoblasts

Shedding of HA occurs mainly via internalization or degradation by hyaluronidases (HYALs) into oligosaccharides [28]. Hence, we examined the expression of human HYALs, a group of enzymes involved in degradation of HA, 24 hpt

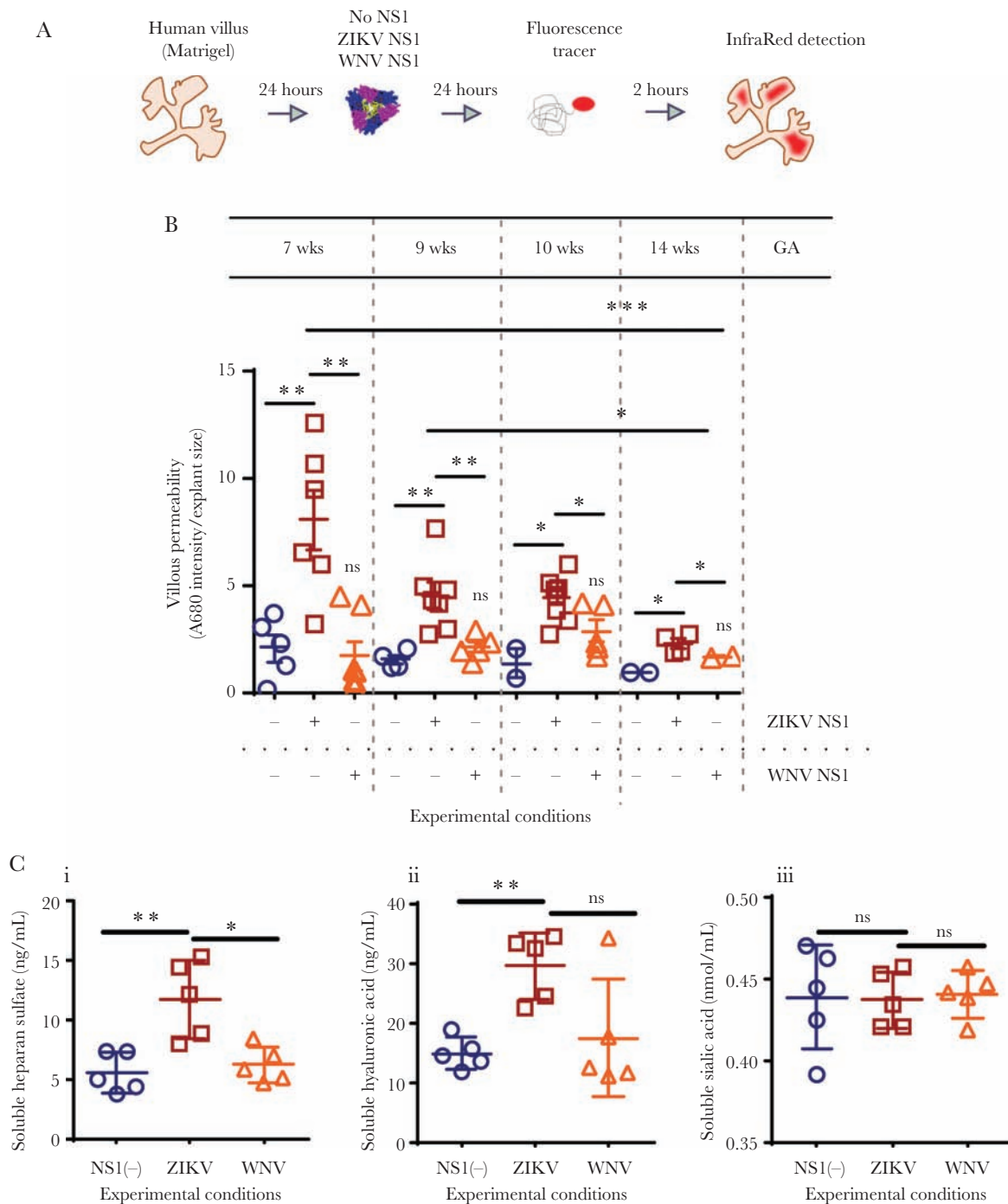


**Figure 3.** Zika virus (ZIKV) NS1 permeabilization and release of glycosaminoglycans in chorionic villous explants. (A and B) Dextran fluorescence permeability of chorionic villous explants treated with exogenous NS1 protein. (A) Chorionic villous explants from 4 different placentas (gestational ages [GA]: 7, 9, 10, and 14 weeks) were treated with ZIKV (open squares) or West Nile virus (WNV) NS1 (open triangles) (5 µg/mL) for 24 hours in the absence of ZIKV. Then, a fluorescence tracer (Dextran A680) was added (100 µg/mL) and 24 hours later, the fluorescence intensity of individual explants was measured using an infrared detection system (LICOR Odyssey CLx Imaging System) and quantified using Image Studio Lite software Version 5.2. Untreated cells (open circles). (B) Raw mean fluorescence intensities (MFIs) were normalized to the cross-sectional area of the explant (MFI/area). Data shown are the MFI/area values for each explant normalized to each explant size, including the mean ± SE. Data were derived from 4 independent experiments and were analyzed by ordinary One-Way analysis of variance and nonparametric Mann-Whitney analysis. \*,  $P < .05$ . \*\*,  $P < .01$ . (C) Enzyme-linked immunosorbent assay quantification of soluble (i) heparan sulfate [HS], (ii) hyaluronic acid [HA], and (iii) sialic acid [Sia] in the supernatants obtained from cultured human chorionic villi 24 hours posttreatment with ZIKV (open squares) or WNV NS1 (open triangles) proteins (5 µg/mL). Untreated cells (open circles). Data were derived from two independent experiments. ns, not significant.

of trophoblasts with NS1 from ZIKV and WNV. We found that ZIKV NS1 stimulated the expression of HYAL on both JAR and JEG-3 cells at 24 hpt (Figure 5A). Notably, HYAL

expression on ZIKV NS1-treated cells was significantly higher than untreated and WNV NS1-treated monolayers and correlated with reduced HA staining (Figure 5A and

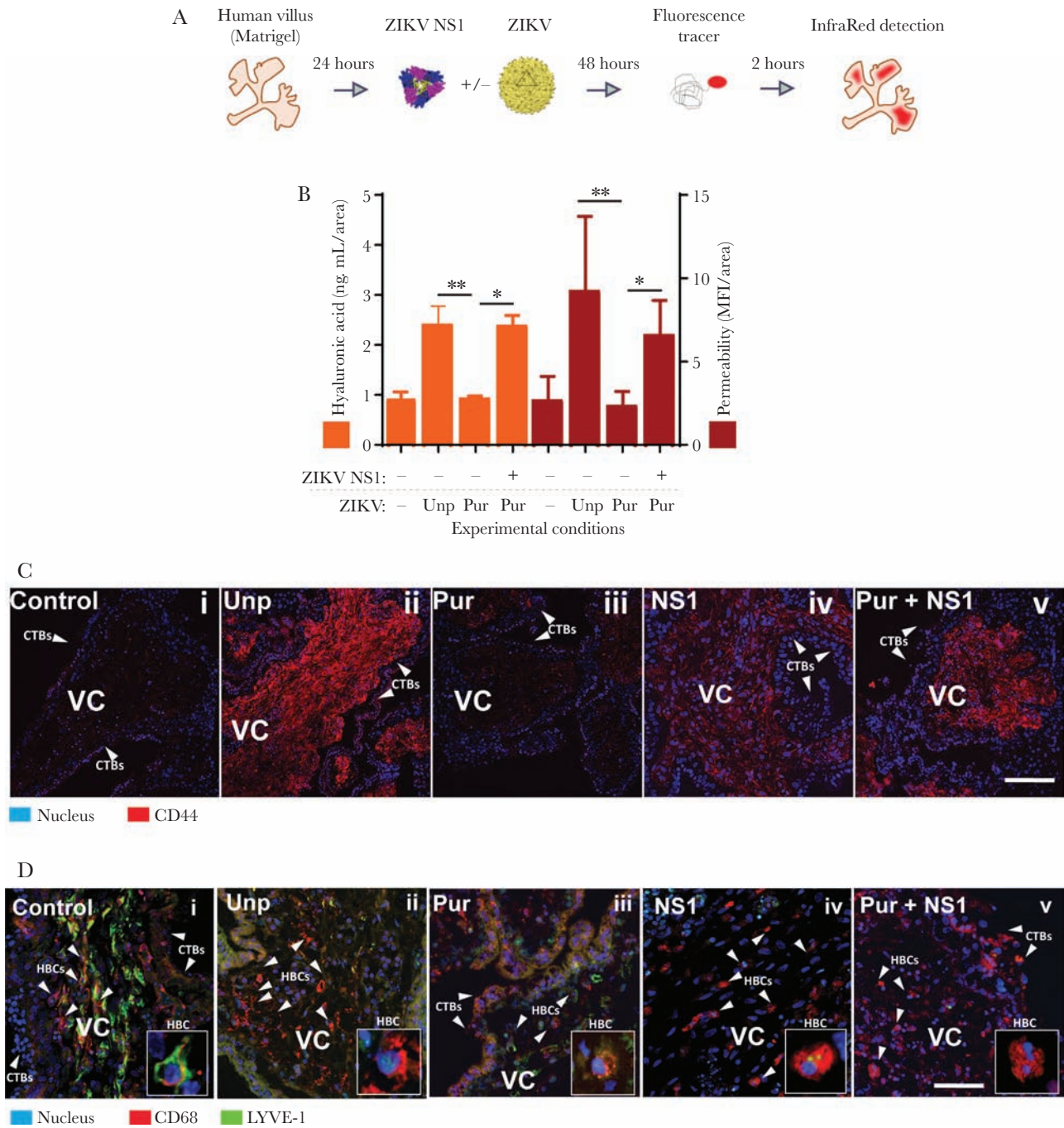


**Figure 4.** Zika virus (ZIKV) in the presence of NS1 induces explant permeability, hyaluronic acid (HA) degradation, and CD44 upregulation in chorionic villous explants. (A and B) Permeability to Alexa680-dextran and levels of HA were measured in chorionic placental explants ( $n = 3$ ) exposed to either unpurified ZIKV (Unp) or purified ZIKV (Pur) in the presence or absence of ZIKV NS1 ( $5 \mu\text{g/mL}$ ) at 2 days postinfection. Raw mean fluorescence intensity (MFI) values were normalized to the cross-sectional area of the explant (MFI/area) (right y-axis). For permeability values, levels of HA (left y-axis) were plotted side-by-side with area-normalized permeability values (right vertical scale). (C and D) Side-by-side immunofluorescent staining of CD44 and lymphatic endothelial cell HA receptor (LYVE)-1 in sections of chorionic villous explants treated and infected as in A and B. Data shown are the MFI/area values for each explant normalized to each explant size, including the mean  $\pm$  standard error. CD68 was used as a marker for fetal macrophages, Hofbauer cells ([HBC] red) (D). Zoomed-in inset depicting expression of CD68 and LYVE-1 in HBCs (lower right). Explants treated only with ZIKV NS1 were also included (iv). Images are representative of 2 independent experiments. Magnification,  $\times 40$ . Scale bar =  $100 \mu\text{M}$ .

B). These results indicate that ZIKV NS1 upregulates the expression of HYALs that could increase HA shedding from trophoblasts.

## DISCUSSION

In previous studies, we and others described the potential routes of ZIKV transmission from mother to fetus using



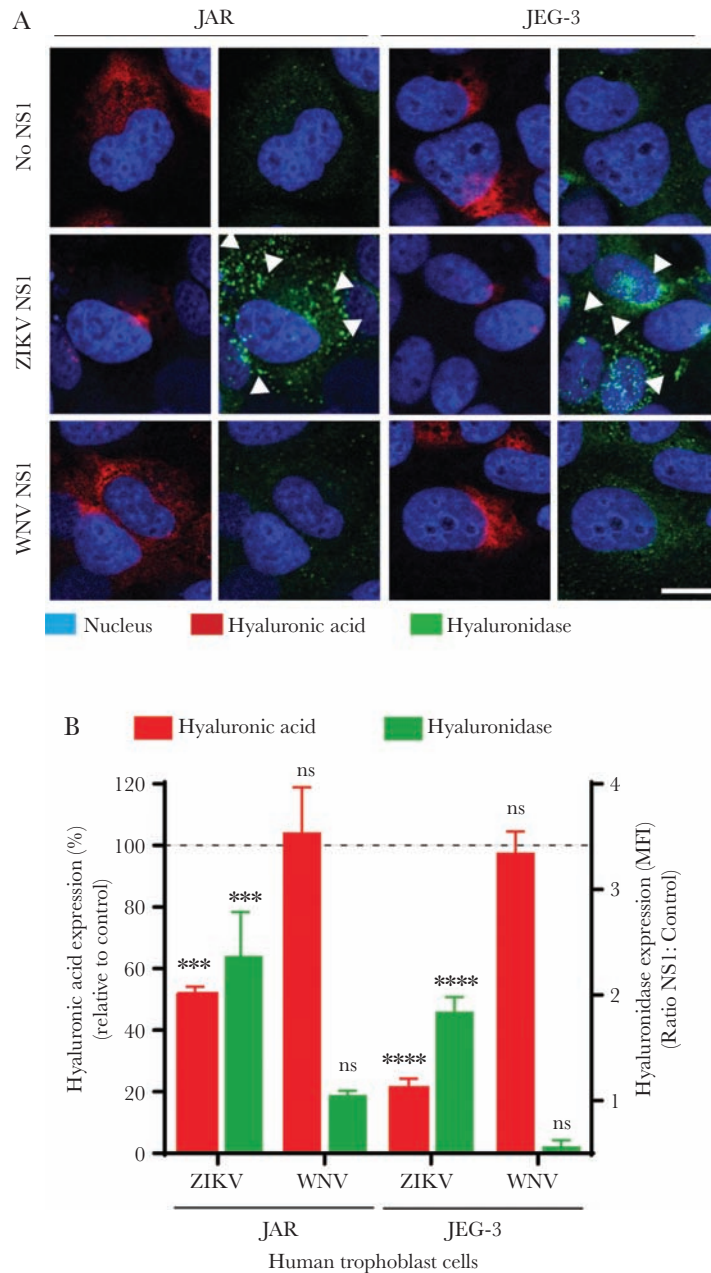


**Figure 5.** Zika virus (ZIKV) NS1 modulates the expression of hyaluronidases in human trophoblast cells. (A) Immunofluorescence staining of hyaluronic acid ([HA, first and third columns) and human hyaluronidase ([HYAL-1, second and fourth columns) in confluent monolayers of JAR and JEG-3 cells cultured on collagen-treated glass coverslips 24 hours posttreatment with ZIKV NS1 (5  $\mu\text{g}/\text{mL}$ ) and West Nile virus (WNV) NS1 (5  $\mu\text{g}/\text{mL}$ ). Images are representative of 2 independent experiments run in duplicate. Magnification,  $\times 20$ . Scale bar = 10  $\mu\text{m}$ . White arrowheads indicate expression of HYAL-1. (B) Mean fluorescence intensity analyses of HA and hyaluronidase expression in JAR and JEG-3 cultures after ZIKV or WNV NS1 treatment as described above. Each bar shows the mean  $\pm$  SE of 2 independent experiments run in duplicate. The percentage of HA expression (dark gray) in JAR and JEG-3 cells treated with NS1 was normalized to the control untreated cells taken as 100%. Hyaluronidase (light gray) was expressed as the ratio (fold change) between NS1 and untreated cells used as control. White arrowheads indicate hyaluronidase expression puncta in trophoblast cells (light gray). Nuclei were stained with Hoechst. Magnification,  $\times 20$ . Scale bars = 5  $\mu\text{m}$ . Ordinary one-way analysis of variance was used for statistical analyses: \*\*\*,  $P < .001$ ; t test, \*\*\*\*,  $P < .0001$  (ZIKV NS1 vs control: JAR and JEG-3 cells). ns, not significant.

anchoring villous explants from human placentas as a model for infection [3, 4, 7, 29, 30]. We have also described the role of flavivirus NS1 in modulating the permeability of human endothelial cell layers, and ZIKV NS1 preferentially triggered hyperpermeability in human umbilical vein endothelial cells

[3, 7]. In this study, we show that ZIKV NS1 modulates the integrity of HS, HA, and Sia, 3 components of the ECM of trophoblast cells, in vitro and in intact villous explants ex vivo, as well as the expression of CD44 and LYVE-1, receptors for soluble HA in the villous core. NS1 induced upregulation of

CD44 in the villous stroma and downregulation of LYVE-1 in Hofbauer cells infected with ZIKV or in the presence of ZIKV NS1 alone. These changes were associated with increased shedding of HA, HS, and Sia and significant disruption of trophoblast and anchoring villus endothelial barrier function. Together, these results highlight ZIKV NS1 as a key viral component that could modulate the permeability of early-gestation placentas targeting cell column CTBs and suggest a potential vaccine target.

The ECM constitutes a network of proteins and GAGs that provides structural support and regulates distinct functional aspects of cell behavior in tissues and organs [31]. In the placenta, GAGs include HS, HA, CS, and the monosaccharide Sia, as well as its large homopolymer form, called polysialic acid, that has been described in the ECM of CTBs and promotes cell motility and penetration of basement membranes [25, 32, 33]. Disruption of GAGs in the ECM under pathophysiological conditions has been shown to lead to impaired barrier function of tissues and increased vascular leakage [7, 8, 12, 34, 35]. In this study, we showed that soluble ZIKV NS1 significantly affects the integrity of HS, HA, and Sia in trophoblasts and anchoring villous explants. Moreover, ZIKV NS1 induced changes in the barrier function of JAR cell monolayers measured by TEER and increased the permeability of villous explants to a fluorescent tracer, dextran-A680. This defective barrier function of human trophoblasts was associated with altered distribution of intercellular junction proteins, such as ZO-1 and E-cadherin, as key components of cell-to-cell contacts. We also found that changes in barrier function of anchoring villi were higher in first-trimester (7 and 9 weeks) compared with later in second-trimester (14 weeks) placentas and were caused by ZIKV NS1 but not NS1 from the closely related WNV. Consistent with this finding, only congenital ZIKV infection has been linked to thousands of cases of birth defects, whereas congenital WNV infection in humans is still sporadic and rare [1, 36, 37]. Our findings suggest that ZIKV NS1, but not WNV NS1, may affect CTB cell columns that are more abundant in first-trimester developing placentas by disrupting the integrity of ECM components [4], potentially leading to persistent infection at the uterine-placenta interface [6]. ZIKV NS1 protein has been detected in the villous core of placentas obtained from ZIKV-infected women [38, 39]. In this study, we found that exposure of anchoring villous explants to ZIKV resulted in hyperpermeability and increased HA. This effect was dependent on the concentration of NS1 in the stock of virus used (unpurified vs purified) and the addition of exogenous ZIKV NS1 to the purified stock of virus. A recent study showed that ZIKV NS1 but not WNV NS1 induced hyperpermeability of human umbilical vein endothelial cells [7]. NS1 is well conserved among flaviviruses, exhibiting 20%–40% identity and 60%–80% similarity [40]. Despite this, ZIKV NS1 possesses divergent electrostatic features that may influence host protein interactions and also ZIKV pathogenesis [41].

As one of the major components of the ECM, HA is a linear, unbranched polysaccharide [27] whose presence is regulated by HYAL-1, the most active somatic HYAL [28]. On tissues, HYALs induce degradation of HA into monosaccharides, accompanied by shedding of HA and subsequent cellular uptake triggered by its binding to CD44 [27] and/or LYVE-1, expressed in the lymphatic endothelium [23]. In this study, a combination of soluble NS1 and ZIKV resulted in increased levels of released HA in explants, which correlated with modulation of the expression of CD44 and LYVE-1 in the villous core. CD44 was highly expressed in explants infected with ZIKV containing either endogenous (unpurified) or exogenous (purified plus recombinant ZIKV NS1) soluble NS1. Increased expression was associated with higher circulating levels of released HA in anchoring villi, suggesting the potential role of soluble HA in modulating CD44 expression. In vitro and in vivo studies have revealed a direct mechanism for HA in promoting cell invasion into sites of inflammation [27, 42–44]. This process was shown to be dependent on both increased levels of CD44-receptor and the removal of HA from the pericellular matrix (ie, fibroblasts) [42, 43]. In eukaryotic cells, shedding of HA can be modulated by hyaluronan synthase or HYAL (HYAL-1), with distinct expression patterns depending on the tissue. In this study, we showed that increased expression of HYAL-1 in 2 human trophoblast cell lines correlated with enhanced shedding of HA in the presence of ZIKV NS1 but not WNV NS1. Recent studies demonstrate activity of HYAL-1 in human placental tissues [45]. As an important proteoglycan-degrading enzyme, altered expression of HYALs may lead to important changes in the composition and structure of GAGs, influencing placental development. Thus, release of HA from anchoring villi, potentially via activation of HYAL-1, may cause upregulation of CD44 expression in villous cores that alters the placental environment. In this study, enzymatic activity for HYAL-1 or HA-synthesis enzymes was not examined. However, determining the contribution of both HYALs and hyaluronan synthases is critical for understanding their potential roles in placental pathology.

Another receptor for soluble HA is LYVE-1, a molecule closely related to the HA receptor CD44 [23]. In this study, in contrast to the increased signal observed for CD44 staining in NS1-treated villi, the levels of LYVE-1 were notably reduced in the villous core of explants infected with unpurified ZIKV, purified ZIKV plus exogenous NS1, or those only exposed to soluble ZIKV NS1 protein. LYVE1 expression was observed on Hofbauer cells, macrophages in the villous core, that were dependent on the presence of NS1 and/or infection [3, 4]. In the placenta, Hofbauer cells can play critical roles in placental vasculogenesis and angiogenesis, immune regulation, and endocrine function across the maternal-fetal barrier [46]. Analysis of ZIKV-infected placentas from congenital infection has revealed proliferation and hyperplasia of Hofbauer cells in second and third trimesters, primarily associated with placental abnormalities leading to congenital malformations

[47–49]. Other studies have demonstrated that arterial macrophages help to maintain normal arterial function via interactions between LYVE-1 and HA [50]. Thus, altered LYVE-1 expression induced by ZIKV NS1 may affect the ability of Hofbauer cells to form and to maintain the vascular structures within the placental villous core, thereby leading to placental dysfunction.

## CONCLUSIONS

In summary, our results suggest that early in gestation, ZIKV could increase NS1 secretion at the uterine-placental interface and alter the normal expression, distribution, and release of important ECM components expressed on STBs and CTBs columns, affecting the expression of specific receptors for glycans (eg, HA) on cells in the chorionic villous stroma of human placentas, such as Hofbauer cells and fibroblasts. This process may alter the permeability and architecture of the placental villi, leading to placental dysfunction and potentially facilitating access of ZIKV into the stromal villous cores, and from there through the endothelial barrier into fetal circulation.

## Supplementary Data

Supplementary materials are available at *The Journal of Infectious Diseases* online. Consisting of data provided by the authors to benefit the reader, the posted materials are not copyedited and are the sole responsibility of the authors, so questions or comments should be addressed to the corresponding author.

**Supplementary Figure 1.** Zika virus (ZIKV) NS1 modulates the expression of glycosaminoglycans (GAGs) on human trophoblast cells. Immunofluorescence staining of (A) heparan sulfate ([HS] green), (B) sialic acid ([Sia] red), and (C) hyaluronic acid ([HA] yellow) on confluent monolayers of JEG-3 cells cultured on collagen-treated glass coverslips 24 hours posttreatment with ZIKV NS1 Suriname (5 µg/mL) or West Nile virus (WNV) NS1 (5 µg/mL). Images are representative of 3 independent experiments run in duplicate. Magnification, ×20. Scale bar = 10 µM.

**Supplementary Figure 2.** Permeability measured by fluorescence assay in chorionic villous explants treated with nonstructural protein 1 (NS1) proteins. (A) Measurement of projected explant area. Explant images imported into Photoshop were outlined using the magic wand tool (1), which selects areas of similar brightness (2). The total number of pixels outlined is recorded using the Record Measurement function, which provides the number of pixels (3). Areas were determined by measuring outlines of images taken on a Leica dissecting scope at ×32. Images were imported directly into Adobe Photoshop, explants were outlined using the magic wand tool, and the total number of pixels within the selected area was recorded using the measurement function in Photoshop (A). For each of 6 experiments with tissue from 6 different placentas, the area-normalized A680 readings were

plotted for each condition, and average values and standard deviations were calculated. (B and C) Explant size and signal intensity. Representative images of human explants treated with Zika virus (ZIKV) or West Nile virus (WNV) NS1 proteins (5 µg/mL) are shown (brightfield). Gestational ages (B) 7 (i–iii) and 9 (iv–vi) weeks, and (C) 10 (i–iii) and 14 (iv–vi) weeks. Scale bars = 0.5 mm.

**Supplementary Figure 3.** Purified Zika virus (ZIKV) has reduced levels of soluble ZIKV nonstructural protein 1 (NS1). Levels of soluble ZIKV NS1 from unpurified (Unp) and purified (Pur) ZIKV preparations used to infect human chorionic villi. Serial dilutions (1:10) of cell-free supernatants of ZIKV-infected C6/36 cells were used to quantify the amount of ZIKV NS1 using an in-house NS1 capture enzyme-linked immunosorbent assay. Levels of NS1 were estimated via linear regression analyses using commercial recombinant ZIKV NS1 (Suriname) to generate an NS1 standard curve. *t* test was used for statistical analyses; \*\*\*, *P* < .0097.

## Notes

**Acknowledgments.** We thank Davide Corti at the Institute for Research in Biomedicine in Bellinzona, Switzerland for kindly donating the anti-ZIKV NS1 monoclonal antibodies used in the NS1-capture enzyme-linked immunosorbent assay.

**Financial support.** This work was funded by grants from the National Institutes of Health Institute for Allergy and Infectious Diseases: R01AI04667 (to L. P.), R21 AI129508 (to L. P. and E. H.), and R01AI124493 (to E. H.).

**Potential conflicts of interest.** All authors: No reported conflicts of interest. All authors have submitted the ICMJE Form for Disclosure of Potential Conflicts of Interest.

## References

1. Mlakar J, Korva M, Tul N, et al. Zika virus associated with microcephaly. *N Engl J Med* **2016**; 374:951–8.
2. Parra B, Lizarazo J, Jiménez-Arango JA, et al. Guillain-Barré syndrome associated with Zika virus infection in Colombia. *N Engl J Med* **2016**; 375:1513–23.
3. Tabata T, Petitt M, Puerta-Guardo H, et al. Zika virus targets different primary human placental cells, suggesting two routes for vertical transmission. *Cell Host Microbe* **2016**; 20:155–66.
4. Tabata T, Petitt M, Puerta-Guardo H, Michlmayr D, Harris E, Pereira L. Zika virus replicates in proliferating cells in explants from first-trimester human placentas, potential sites for dissemination of infection. *J Infect Dis* **2018**; 217:1202–13.
5. Bayer A, Lennemann NJ, Ouyang Y, et al. Type III interferons produced by human placental trophoblasts confer protection against Zika virus infection. *Cell Host Microbe* **2016**; 19:705–12.
6. Pereira L. Congenital viral infection: traversing the uterine-placental interface. *Annu Rev Virol* **2018**; 5:273–99.

7. Puerta-Guardo H, Glasner DR, Espinosa DA, et al. Flavivirus NS1 triggers tissue-specific vascular endothelial dysfunction reflecting disease tropism. *Cell Rep* **2019**; 26:1598–613.e8.
8. Glasner DR, Ratnasiri K, Puerta-Guardo H, Espinosa DA, Beatty PR, Harris E. Dengue virus NS1 cytokine-independent vascular leak is dependent on endothelial glycocalyx components. *PLoS Pathog* **2017**; 13:e1006673.
9. Puerta-Guardo H, Glasner DR, Harris E. Dengue virus NS1 disrupts the endothelial glycocalyx, leading to hyperpermeability. *PLoS Pathog* **2016**; 12:e1005738.
10. Glasner DR, Puerta-Guardo H, Beatty PR, Harris E. The good, the bad, and the shocking: the multiple roles of dengue virus nonstructural protein 1 in protection and pathogenesis. *Annu Rev Virol* **2018**; 5:227–53.
11. Tang TH, Alonso S, Ng LF, et al. Increased serum hyaluronic acid and heparan sulfate in dengue fever: association with plasma leakage and disease severity. *Sci Rep* **2017**; 7:46191.
12. Suwanto S, Sasmono RT, Sinto R, Ibrahim E, Suryamin M. Association of endothelial glycocalyx and tight and adherens junctions with severity of plasma leakage in dengue infection. *J Infect Dis* **2017**; 215:992–9.
13. Gandhi NS, Mancera RL. The structure of glycosaminoglycans and their interactions with proteins. *Chem Biol Drug Des* **2008**; 72:455–82.
14. Chen Y, Maguire T, Hileman RE, et al. Dengue virus infectivity depends on envelope protein binding to target cell heparan sulfate. *Nat Med* **1997**; 3:866–71.
15. Gao H, Lin Y, He J, et al. Role of heparan sulfate in the Zika virus entry, replication, and cell death. *Virology* **2019**; 529:91–100.
16. Schauer R. Sialic acids as regulators of molecular and cellular interactions. *Curr Opin Struct Biol* **2009**; 19:507–14.
17. Varki A. Biological roles of glycans. *Glycobiology* **2017**; 27:3–49.
18. Zhu R, Huang YH, Tao Y, et al. Hyaluronan up-regulates growth and invasion of trophoblasts in an autocrine manner via PI3K/AKT and MAPK/ERK1/2 pathways in early human pregnancy. *Placenta* **2013**; 34:784–91.
19. Zhu R, Wang SC, Sun C, et al. Hyaluronan-CD44 interaction promotes growth of decidual stromal cells in human first-trimester pregnancy. *PLoS One* **2013**; 8:e74812.
20. Misra S, Hascall VC, Markwald RR, Ghatak S. Interactions between hyaluronan and its receptors (CD44, RHAMM) regulate the activities of inflammation and cancer. *Front Immunol* **2015**; 6:201.
21. Red-Horse K, Rivera J, Schanz A, et al. Cytotrophoblast induction of arterial apoptosis and lymphangiogenesis in an in vivo model of human placentation. *J Clin Invest* **2006**; 116:2643–52.
22. Tabata T, Pettitt M, Fang-Hoover J, et al. Cytomegalovirus impairs cytotrophoblast-induced lymphangiogenesis and vascular remodeling in an in vivo human placentation model. *Am J Pathol* **2012**; 181:1540–59.
23. Banerji S, Ni J, Wang SX, et al. LYVE-1, a new homologue of the CD44 glycoprotein, is a lymph-specific receptor for hyaluronan. *J Cell Biol* **1999**; 144:789–801.
24. Stettler K, Beltramello M, Espinosa DA, et al. Specificity, cross-reactivity, and function of antibodies elicited by Zika virus infection. *Science* **2016**; 353:823–6.
25. Rothbauer M, Patel N, Gondola H, Siwetz M, Huppertz B, Ertl P. A comparative study of five physiological key parameters between four different human trophoblast-derived cell lines. *Sci Rep* **2017**; 7:5892.
26. Srinivasan B, Kolli AR, Esch MB, Abaci HE, Shuler ML, Hickman JJ. TEER measurement techniques for in vitro barrier model systems. *J Lab Autom* **2015**; 20:107–26.
27. Knudson W, Chow G, Knudson CB. CD44-mediated uptake and degradation of hyaluronan. *Matrix Biol* **2002**; 21:15–23.
28. Stern R, Jedrzejewski MJ. Hyaluronidases: their genomics, structures, and mechanisms of action. *Chem Rev* **2006**; 106:818–39.
29. Hermanns K, Göhner C, Kopp A, et al. Zika virus infection in human placental tissue explants is enhanced in the presence of dengue virus antibodies in-vitro. *Emerg Microbes Infect* **2018**; 7:198.
30. Platt DJ, Smith AM, Arora N, Diamond MS, Coyne CB, Miner JJ. Zika virus-related neurotropic flaviviruses infect human placental explants and cause fetal demise in mice. *Sci Transl Med* **2018**; 10:eaao7090.
31. Frantz C, Stewart KM, Weaver VM. The extracellular matrix at a glance. *J Cell Sci* **2010**; 123:4195–200.
32. Fried M, Duffy PE. Adherence of *Plasmodium falciparum* to chondroitin sulfate A in the human placenta. *Science* **1996**; 272:1502–4.
33. Hromatka BS, Drake PM, Kapidzic M, et al. Polysialic acid enhances the migration and invasion of human cytotrophoblasts. *Glycobiology* **2013**; 23:593–602.
34. Kim YH, Nijst P, Kiefer K, Tang WH. Endothelial glycocalyx as biomarker for cardiovascular diseases: mechanistic and clinical implications. *Curr Heart Fail Rep* **2017**; 14:117–26.
35. Reitsma S, Slaaf DW, Vink H, van Zandvoort MA, oude Egbrink MG. The endothelial glycocalyx: composition, functions, and visualization. *Pflugers Arch* **2007**; 454:345–59.
36. Rasmussen SA, Jamieson DJ, Honein MA, Petersen LR. Zika virus and birth defects—reviewing the evidence for causality. *N Engl J Med* **2016**; 374:1981–7.
37. Centers for Disease Control and Prevention (CDC). Intrauterine West Nile virus infection—New York, 2002. *MMWR Morb Mortal Wkly Rep* **2002**; 51:1135–6.

38. Rabelo K, de Souza Campos Fernandes RC, de Souza LJ, et al. Placental histopathology and clinical presentation of severe congenital Zika syndrome in a human immunodeficiency virus-exposed uninfected infant. *Front Immunol* **2017**; 8:1704.
39. Rosenberg AZ, Yu W, Hill DA, Reyes CA, Schwartz DA. Placental pathology of Zika virus: viral infection of the placenta induces villous stromal macrophage (Hofbauer cell) proliferation and hyperplasia. *Arch Pathol Lab Med* **2017**; 141:43–8.
40. Xu X, Vaughan K, Weiskopf D, et al. Identifying candidate targets of immune responses in Zika virus based on homology to epitopes in other flavivirus species. *PLoS Curr.* **2016**; 8. pii: ecurrents.outbreaks.9aa2e1fb61b0f632f58a098773008c4b
41. Song H, Qi J, Haywood J, Shi Y, Gao GF. Zika virus NS1 structure reveals diversity of electrostatic surfaces among flaviviruses. *Nat Struct Mol Biol* **2016**; 23:456–8.
42. Kim Y, Kumar S. CD44-mediated adhesion to hyaluronic acid contributes to mechanosensing and invasive motility. *Mol Cancer Res* **2014**; 12:1416–29.
43. Tzircotis G, Thorne RF, Isacke CM. Chemotaxis towards hyaluronan is dependent on CD44 expression and modulated by cell type variation in CD44-hyaluronan binding. *J Cell Sci* **2005**; 118:5119–28.
44. DeGrendele HC, Estess P, Siegelman MH. Requirement for CD44 in activated T cell extravasation into an inflammatory site. *Science* **1997**; 278:672–5.
45. Yamada M, Hasegawa E, Kanamori M. Purification of hyaluronidase from human placenta. *J Biochem* **1977**; 81:485–94.
46. Seval Y, Korgun ET, Demir R. Hofbauer cells in early human placenta: possible implications in vasculogenesis and angiogenesis. *Placenta* **2007**; 28:841–5.
47. Kim JS, Romero R, Kim MR, et al. Involvement of Hofbauer cells and maternal T cells in villitis of unknown aetiology. *Histopathology* **2008**; 52:457–64.
48. Toti P, Arcuri F, Tang Z, et al. Focal increases of fetal macrophages in placentas from pregnancies with histological chorioamnionitis: potential role of fibroblast monocyte chemoattractant protein-1. *Am J Reprod Immunol* **2011**; 65:470–9.
49. de Noronha L, Zanluca C, Burger M, et al. Zika virus infection at different pregnancy stages: anatomopathological findings, target cells and viral persistence in placental tissues. *Front Microbiol* **2018**; 9:2266.
50. Lim HY, Lim SY, Tan CK, et al. Hyaluronan receptor LYVE-1-expressing macrophages maintain arterial tone through hyaluronan-mediated regulation of smooth muscle cell collagen. *Immunity* **2018**; 49:1191.